ORGANIC PROCESS RESEARCH & DEVELOPMENT
OPR&D
Article
pubs.acs.org/OPRD

Downstream Processability of Crystal Habit-Modified Active Pharmaceutical Ingredient

Nawin Pudasaini,[†] Pratik P. Upadhyay,[†] Christian R. Parker,[‡] Stefan U. Hagen,[‡] Andrew D. Bond,[†,§] and Jukka Rantanen*,[†]

[†]Department of Pharmacy, Faculty of Health and Medical Sciences, University of Copenhagen, Universitetsparken 2, Copenhagen, Denmark

[‡]Syntese A/S, Industriholmen 11-13, Hvidovre, Denmark

[§]Department of Chemistry, University of Cambridge, Cambridge, U.K.

Supporting Information

ABSTRACT: Efficient downstream processing of active pharmaceutical ingredients (APIs) can depend strongly on their particulate properties, such as size and shape distributions. Especially in drug products with high API content, needle-like crystal habit of an API may show compromised flowability and tabletability, creating significant processability difficulties on a production scale. However, such a habit can be adapted to the needs of downstream processing. To this end, we modified the needle-like crystal habit of the model API 5-aminosalicylic acid (5-ASA). This study reports processability assessment of six representative crystal habits of 5-ASA (needles, plates, rectangular bars, rhombohedrals, elongated hexagons, and spheroids) in the context of direct compression using ring shear tester, flow rate analyzer, and instrumented tablet press. As expected, needles were very cohesive, had low flow rate (1.0 ± 0.08 mg/s), and low bulk density (0.14 ± 0.01 g/mL) but showed better tabletability, whereas the opposite was observed with more isotropic crystal habits. For instance, spheroids, elongated hexagons, and rhombohedrals were easy/free-flowing and had high bulk densities ($\geq$0.5 g/mL), but final tablets had lower tensile strength than that of needles. Of the six crystal habits, the plates showed a good compromise considering both flowability and tabletability.

1. INTRODUCTION

Oral solid dosage forms constitute a major share of drug products manufactured across pharmaceutical industries.[1] Such dosage forms are produced from heterogeneous powder blends containing an active pharmaceutical ingredient (API), where it typically contributes between 5 and 90% to the overall weight of the drug products. In the drug products with high API content, particulate properties of an API determine the manufacturing processes to be used for downstream processing.[2,3] For tablet manufacturing, direct compression (DC) is preferred over more complicated dry or wet granulation.[4] However, DC demands good flowability and tabletability of powder blends. Furthermore, with the U.S. Food and Drug Administration (FDA) encouraging pharmaceutical industries to modernize small-molecule manufacturing using continuous manufacturing concepts,[5] DC makes the continuous manufacturing line much simpler[6] with just two processing steps (blending and compression). To that end, particulate properties of an API must enable its DC. Although much effort is paid to control crystal forms and size distributions of an API, the crystal habit is often overlooked during "pure" polymorph screening. However, crystal habits can be adapted to the needs of downstream processing.

In general terms, a crystal habit refers to the external appearance of a crystal and has been used interchangeably with crystal shape or crystal morphology. The crystal habit of an API is known to influence its physicochemical,[7] biopharmaceutical,[8] and mechanical properties.[9] Many APIs with anisotropic crystal habits, such as needles or flakes, present significant difficulties in downstream processing and can be difficult to formulate into solid dosage forms due to its compromised flowability and tabletability.[10] Generally, such processability challenges are overcome either by using large quantities of functional excipients or with additional processing steps like milling, granulation, as well as roller compaction. However, increasing excipient quantity can result in large-sized dosage forms and can negatively impact patient compliance.[11] Furthermore, excipient overload may not cover the poor API properties in high drug load formulations. Additional corrective processing steps increase manufacturing costs as they incur more resources, energy, control, and time and can be deleterious to API physical stability. Consequently, eliminating non-value-adding operations has obvious advantages.

API properties responsible for its bulk behavior such as its solid forms, crystal size, and crystal habit can be predefined during the crystallization step. Extensive efforts have been made in understanding the API crystal growth and on the predictability of their crystal habits.[12] In addition, several methods are established to manipulate crystal habits.[13] These broadly include changing recrystallization solvents, the use of "tailor-made" small-molecule additives, or different types of macromolecules. However, such investigations typically end with generating multiple crystal habits and, very rarely, focus on identifying optimal habits for efficient downstream processing. Identifying an optimal crystal habit is essential; after all,

Received: December 21, 2016
Published: March 2, 2017

DOI: 10.1021/acs.oprd.6b00434
Org. Process Res. Dev. XXXX, XXX, XXX−XXX

different processes can demand different habits. For instance, isotropic shapes flow better,[14] whereas such habits may not be optimal for tableting. With the availability of material-sparing instruments for processability assessment, such evaluation can be carried out in the laboratory phase of product development.

This paper reports processability assessment of different crystal habits of the model API 5-aminosalicylic acid (5-ASA). As an anti-inflammatory agent, 5-ASA is used to treat inflammatory bowel diseases, which crystallizes out as needles under its typical crystallization conditions. To improve its downstream processability, we obtained alternative crystal habits of 5-ASA. This study is aimed at identifying the optimal crystal habit of 5-ASA in the context of direct compression.

2. EXPERIMENTAL SECTION

5-Aminosalicylic acid (5-ASA, $C_7H_7NO_3$, MW 153.14), the API for Mesalazine, was kindly donated by Syntese A/S (Denmark). It was crystallized in six different crystal habits (needles, plates, rectangular bars, elongated hexagons, rhombohedrals, and spheroids). All habit-modified 5-ASA was obtained by recrystallization using pH and temperature change techniques and applying small amounts of additives. The exact conditions and methods for preparing such habits are outside the scope of this article.

2.1. Powder X-ray Diffraction (PXRD). PXRD was collected on a PANalytical X'Pert Pro instrument equipped with a PIXcel detector using nonmonochromatic Cu Kα radiation (λ_{avg} = 1.5418 Å) at 40 kV and 40 mA. Samples were measured in the reflection geometry from 4 to 40° 2θ. The diffraction patterns were compared with its reference pattern generated using the software Mercury[15] 3.8 from its crystal structure (reference code: SAQVAJ[16]), which was taken from The Cambridge Structural Database (CSD).[17]

2.2. Crystal Shape and Size Distributions. An automated image analysis system (Morphologi G2, Malvern Instruments, U.K.) consisting of an optical microscope and image analysis software (Morphologi 8.21) was used to determine crystal size and shape distributions. Crystals (10–25 mg) were suspended in oil (Myglyol), stirred, and sonicated. A drop of suspension was placed on a glass slide, and multiple images were taken. From the images of each crystal, ten different size- and shape-related parameters were calculated. Size-related parameters included circle equivalent diameter, area, length, width, and perimeter, and shape-related parameters included aspect ratio, high sensitive circularity (HS circularity), solidity, convexity, and circularity. These terms are defined in the Table SI 1. Additionally, crystals were also visualized using a tabletop scanning electron microscope (TM3030 Hitachi, Japan).

2.3. Principal Component Analysis. We used principal component analysis (PCA; SIMCA 14.1; MKS Umetrics, Sweden) to compare six crystal populations considering all shape- and size-related parameters, treating them as variables. Variables were given equal weight using the univariate method before PCA modeling. PCA is a multivariate method where multidimensional data are projected into a few orthogonal features called principal components. The components are fewer than variables, and thereby, complexity is reduced. Components describe the variation in the data set where the first component explains the largest variation, whereas the second component describes the second largest variation, and so on. More details about PCA and its similar applications can be found in the literature.[18,19]

2.4. Powder Flow Properties Assessment. We assessed powder flow properties using a ring shear tester (RST-XS, Dietmar Schulze, Germany) and flow rate analyzer (FlowPro, SAY group Oy, Finland). Figures of both the instruments are included in the Supporting Information (Figures SI 2 and SI 4). All of the measurements were performed in triplicate at 22 ± 2 °C and 25–40% relative humidity. For flow behavior using flowability index and flow rates to be defined, powders were classified into different categories, as in Table 1.

Table 1. Classification Scheme Used for Defining Flow Behavior Using Flowability Index and Flow Rates in This Study[a]

flowability index		flow rate	
$1 \le ffc$	not flowing	<10 mg/s	poorly flowing
$1 < ffc \le 2$	very cohesive	10–100 mg/s	intermediate flowing
$2 < ffc \le 4$	cohesive	>100 mg/s	free-flowing
$4 < ffc \le 10$	easy flowing		
$10 < ffc$	free-flowing		

[a]"Flowability index" classification is similar to Jenike's classification scheme,[20] and "flow rate" classification is based on the work of Seppala et al.[21]

Flowability index (ffc), bulk density (ρ_b), and effective angle of internal friction (φ_e) were determined by measuring shear stress needed to overcome internal friction in powders with ring shear tester following a standard procedure[22] in the shear cell XS-SV3 (volume = 3.5 cm^3). Powders were first presheared to steady-state consolidation with 1 kPa pressure, and subsequently, four normal stresses (300, 467, 633, and 800 Pascals) were applied to measure corresponding shear stress. Further discussion on how ffc, ρ_b, and φ_e were determined is in the Supporting Information. In addition, flow rates (milligrams per second, mg/s) were measured with a flow rate analyzer, whose detailed description can be found elsewhere.[21] The slope of a mass function, which is a plot of the cumulative amount of powder (mg) flowing out of an orifice as a function of time, was used to calculate flow rates.

2.5. Tabletability. Cylindrical flat-faced compacts of 6 mm diameter were prepared on a calibrated benchtop instrumented tablet press (Gamlen Tableting Ltd., UK) equipped with a 500 kg load cell (CT6-500-022). Powders (100 ± 10 mg) were compacted at 35, 71, 106, 142, and 180 MPa pressures with a compression speed of 60 mm/min. Before compression, the punch tip and die wall were lubricated with magnesium stearate suspension made in acetone. Eq 1 as proposed by Fell[23] was used to calculate the tablet tensile strength (σ_t, MPa) for cylindrical tablets.

$$\sigma_t = 2F/\pi Dt \quad (1)$$

where F represents the breaking force (N), D is the diameter (mm), and t is the thickness (mm) of the tablet. Breaking force (the diametrical force required to break the tablet) was measured in the same compaction simulator but using a 50 kg load cell (CT050-012). Tablets for each compaction pressure were prepared in triplicate.

3. RESULTS AND DISCUSSION

Under typical crystallization conditions, 5-ASA crystallizes out as needles. Such a crystal habit can significantly compromise its downstream processability. With the aim of adapting the crystal habit to the needs of downstream processing and handling, 5-

DOI: 10.1021/acs.oprd.6b00434
Org. Process Res. Dev. XXXX, XXX, XXX–XXX

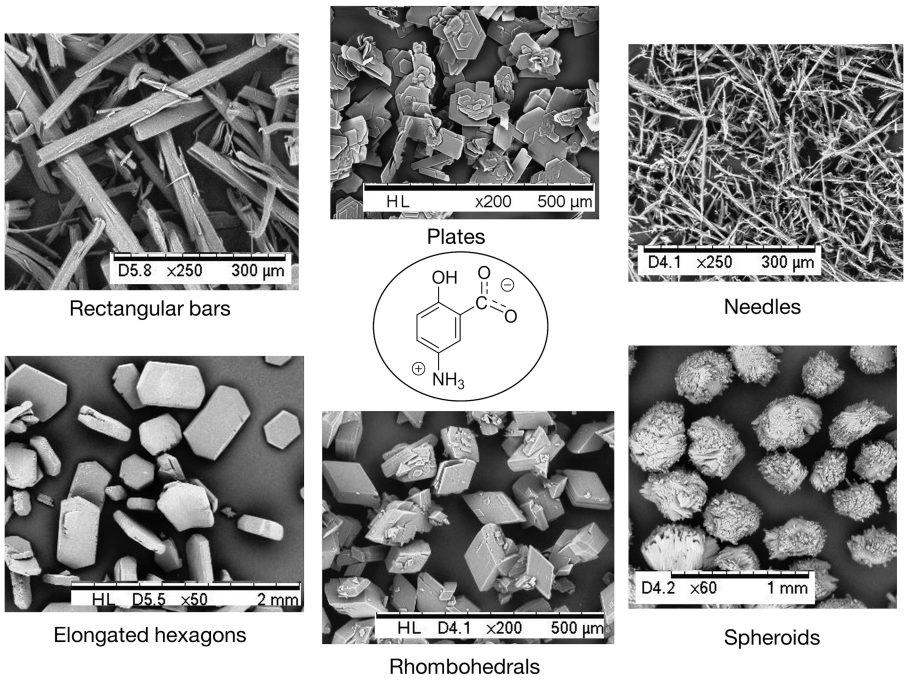

Figure 1. Scanning electron microscopic images of six crystal habits of 5-ASA. The 5-ASA structure formula, in its zwitterionic state, is at the center (note different size scales in the images).

ASA was crystallized in different habits. This study reports processability assessment, based on bulk powder flowability and tabletability, of six representative crystal habits (Figure 1): needles, rectangular bars, plates, rhombohedrals, elongated hexagons, and spheroids.

3.1. Solid-State Analysis of Crystals. *Powder X-ray Diffraction (PXRD).* In general, crystal habit modification results from altering crystal growth conditions or through polymorphic transformations.[24] When growth conditions are identical, different polymorphs may show different habits. This essentially limits the scope of habit modification, particularly if new polymorphs crystallizing are thermodynamically less stable. This is generally an issue because different polymorphic forms are known to exhibit significant bioavailability differences and can have detrimental effect on its clinical effectiveness.

Although to date 5-ASA is known to exist as single polymorphs (CSD version 5.38),[17] new polymorphs may result from the conditions used for habit modification. Because the focus was on the processability of the various morphologies of the same polymorphs and because polymorphs can differ in their mechanical properties,[25] we recorded PXRD patterns to rule out the polymorphic transformation. No polymorphic transformation was observed as the PXRD pattern of each habit matched (Figure 2) with the reference pattern.

Crystal-Size and Shape Distributions. Usually, the particle size and shape distributions are described by a single point value with deviations and distribution span as in Table 2. Such conventional practice works when the comparison is based on a single parameter and when all other parameters do not vary. For instance, describing two or more needle-shaped particle populations can be sufficient with its size such as D_{50}. As is the case in our study, complexities arise when both shape and size vary together. For such complexity to be circumvented, PCA was employed. PCA provides an intuitive presentation of hidden data patterns with two plots, namely, score and loading plots. The score plot yields information regarding sample

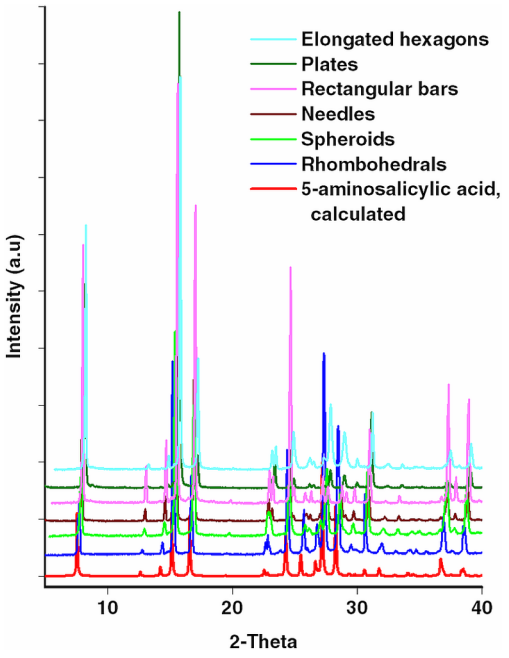

Figure 2. Powder X-ray diffraction pattern of habit-modified 5-ASA. Reference pattern generated from 5-ASA crystal structure (CSD reference code: SAQJAV).[16]

groupings, their similarities, and dissimilarities based on all parameters, whereas the loading plot separates the variables responsible for patterns in the score plot.

Using PCA, ten variables were reduced to three principal components explaining 94.5% of the variations in the data set. The score plot in Figure 3 shows how each crystal population relates to each other when all ten parameters are considered. Six habits cluster in different regions, indicating expected differences between crystal populations. The rhombohedral habit overlapped with plates, showing their similarities in terms

DOI: 10.1021/acs.oprd.6b00434
Org. Process Res. Dev. XXXX, XXX, XXX−XXX

Table 2. Crystal Shape and Size Distributions of Six Different Crystal Habits of 5-ASA[a]

		shape-related parameters					CE diameter (μm)			size-related parameters			
crystal habit	no. of crystals	aspect ratio (M ± SD)	circularity (M ± SD)	convexity (M ± SD)	solidity (M ± SD)	HS circularity (M ± SD)	D_{10}	D_{50}	D_{90}	length (M ± SD) (μm)	width (M ± SD) (μm)	perimeter (μm)	area (μm^2)
needles	4180	0.18 ± 0.06	0.49 ± 0.08	0.96 ± 0.03	0.78 ± 0.13	0.26 ± 0.09	14.94	18.39	27.4	58.1 ± 22.7	9.75 ± 3.1	126.2	356.4
rectangular bars	3688	0.22 ± 0.1	0.59 ± 0.09	0.98 ± 0.03	0.89 ± 0.11	0.35 ± 0.12	17.5	34.1	81.1	106.7 ± 80.3	20.7 ± 14.3	236.5	2089.3
plates	4229	0.71 ± 0.15	0.85 ± 0.07	0.95 ± 0.06	0.95 ± 0.04	0.73 ± 0.12	19.94	41.5	93.9	63.8 ± 37.4	45.9 ± 29.3	186.5	2698.8
rhombohedrals	2053	0.6 ± 0.11	0.87 ± 0.04	0.97 ± 0.02	0.96 ± 0.03	0.76 ± 0.07	24.53	50.2	96.7	75.8 ± 40.6	50.2 ± 26.4	201.7	3402.1
elongated hexagons	1464	0.76 ± 0.12	0.91 ± 0.04	0.97 ± 0.03	0.97 ± 0.03	0.83 ± 0.07	232.65	369.15	482.1	432.8 ± 122.9	321.8 ± 78.2	1257.3	112224.8
spheroids	767	0.63 ± 0.14	0.86 ± 0.07	0.95 ± 0.05	0.95 ± 0.04	0.74 ± 0.11	272.26	542.36	770.3	723.6 ± 295.6	434.7 ± 167.8	2007.2	262045.7
MCC 102	**357**	**0.54 ± 0.17**	**0.76 ± 0.07**	**0.95 ± 0.04**	**0.89 ± 0.05**	**0.58 ± 0.11**	**28.95**	**50.8**	**102.81**	**94.43 ± 52.41**	**49.36 ± 30.34**	**240.98**	**3702.6**

[a]Each parameter is defined in Table SI 1. M and SD represent mean and standard deviations, respectively. Corresponding values for reference (microcrystalline cellulose PH 102, MCC 102) are also shown.

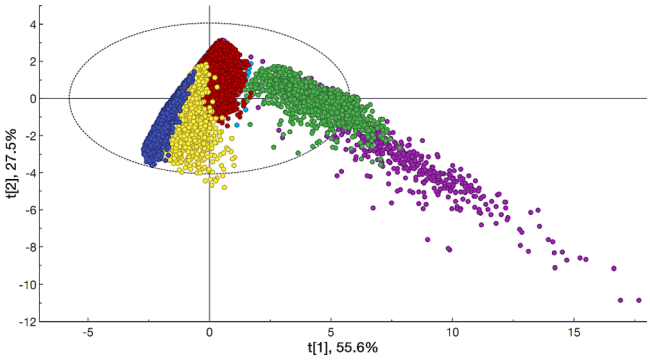

Figure 3. Principal component analysis (PCA) score plot to visualize six crystal habits based on shape- and size-related parameters. The percent values in the axes titles indicate variation explained by the respective component. Colors: needles (dark blue), rectangular bars (yellow), plates (red), rhombohedrals (sky blue, masked by plates), elongated hexagons (green), and spheroids (purple).

of both size- and shape-related parameters. The loading plot in Figure 4 shows the size-related parameters dominated the first

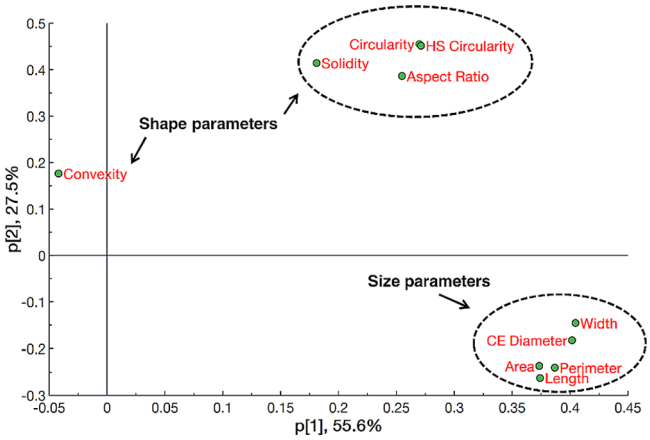

Figure 4. Principal component analysis (PCA) loading plot indicating the importance of different size- and shape-related parameters for the first two components. The percent values in the axes titles indicate variation explained by the respective components.

component and accounted for 55.6% of the variance. The second and third components were influenced by shape-related parameters. Although PCA provided visual insight into similarities or differences among six crystal habit populations, it does not characterize crystal shape and size as such.

3.2. Flow Properties Assessment. The ring shear tester and FlowPro were used to evaluate powder flow parameters (flowability index, bulk density, effective angle of internal friction properties, and flow rates). The same flow parameters were also measured for microcrystalline cellulose PH 102 (MCC 102) included as a reference. MCC 102 is a pharmaceutical excipient known to possess good flow properties.[14] As powder flowability is a complex function of material physical properties and the equipment used to handle, store, or process the materials, the equipment-related effects were fixed using stress normally prevalent in a 20 L hopper of small-scale tablet machines.[26]

Figure 5 shows the flowability index and flow rates of six habits of 5-ASA together with MCC 102. In general, a similar trend and order of powder flow were observed with both

DOI: 10.1021/acs.oprd.6b00434
Org. Process Res. Dev. XXXX, XXX, XXX−XXX

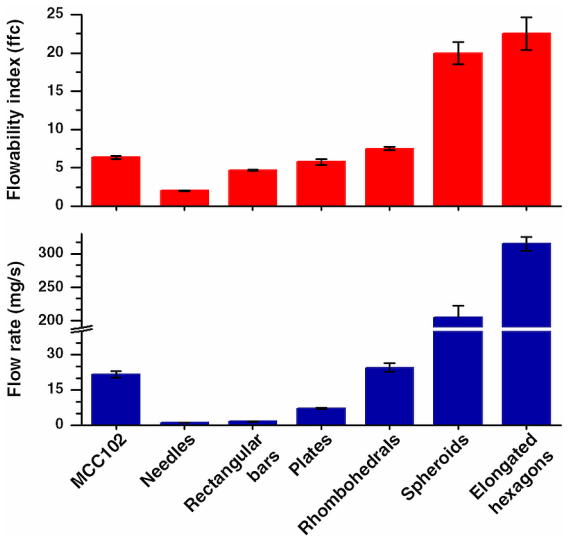

Figure 5. Flowability index (top, ff_c, dimensionless) and flow rates (bottom, mg/s) of six crystal habits of 5-ASA. Microcrystalline cellulose (MCC PH102) is also shown for comparison. Data are mean values of three measurements. The horizontal axes for lower and upper bar graphs are the same.

methods. On the basis of the flowability index, needles were identified as very cohesive ($ff_c \leq 2$), spheroids and elongated hexagons as free flowing ($ff_c > 10$), and the rest as easy flowing. On the basis of the flow rates, needles, rectangular bars, and plates were identified as poorly flowing (flow rate < 10 mg/s), and spheroids as well as elongated hexagons were identified as free flowing (flow rate > 100 mg/s). Furthermore, when compared to MCC 102, all habits, except needles and rectangular bars, had similar or higher flowability index, but when flow rates are compared, rhombohedrals, spheroids, and elongated hexagons had better flow rates than that of MCC 102. Although the flowability index of MCC 102 can vary with relative humidity, the value measured in this study was 6.3 ± 0.19, which is similar to the experimentally determined value under similar conditions.[27]

Table 3 presents bulk density (ρ_b) and effective angle of internal friction (φ_e) of six habits of 5-ASA. Both bulk density and effective angle of internal friction are dependent on consolidation stress. For the same consolidation stress, higher values of φ_e indicate a cohesive nature. Physically, a high value for φ_e gives an indication of stronger interparticle interactions. Needles had the lowest ρ_b and highest φ_e, indicating their cohesive nature, whereas rhombohedrals, spheroids, and elongated hexagons had bulk densities greater than 0.5 g/mL and φ_e were less than 40°. Sirola et al. reported similar bulk density (0.15−0.25 g/mL) for their needle-shaped 5-ASA.[28]

Table 3. Bulk Density (g/mL) and Effective Angle of Internal Friction (deg) Determined Using Ring Shear Tester at 1000 Pascal Consolidation Stress (Mean ± SD for n = 3)

crystal habits	bulk density (ρ_b) (g/mL)	effective angle of internal friction (φ_e) (deg)
needles	0.14 ± 0.003	49.6 ± 1.2
plates	0.19 ± 0.007	37.3 ± 0.6
rectangular bars	0.27 ± 0.004	40.4 ± 0.9
rhombohedrals	0.54 ± 0.009	36.1 ± 0.2
spheroids	0.53 ± 0.007	35.8 ± 1.0
elongated hexagons	0.63 ± 0.007	32.5 ± 0.5

Achieving proper powder flow is critical to many downstream pharmaceutical processes such as blending, transfer, storage, feeding, fluidization, tableting, and capsule filling. Performing flowability assessment of an API early in product development is therefore recommended. This can be carried out with the availability of material-sparing instruments.[29,30] For instance, in our case, flow property evaluation only needs 3−8 g of powder depending on the bulk density. The results of flowability assessment showed when 5-ASA crystals gradually became more isotropic (aspect ratio > 0.5) and larger (Table 2), the powder flow improved as indicated by high values of flow parameters. Elongated hexagons and spheroids were found to have the best flow properties, whereas rhombohedrals exhibited flow properties comparable to those of MCC 102.

3.3. Tabletability Assessment. The tableting performance is typically assessed with a tabletability plot, which illustrates the effect of increasing compaction pressure on tablet tensile strength. The tablet tensile strength is a measure of the mechanical strength of a compact. At the same compaction pressure, a tablet with higher tensile strength indicates better ability of the powder to form intact tablets. In general, tablets tensile strength should be adequate to withstand stress encountered during postcompression unit operations, namely, coating, packaging, during transport, and in end-use by the patients, whereas it should not be too high that it fails the disintegration test. Literature suggests diverse views regarding adequate tensile strength for tablets.[2,3,31,32] As a general guide, tensile strength ≥ 1.7 MPa at a solid fraction < 0.9 is typically sufficient for tablets to be robust for handling during further processing. However, tensile strength down to 1 MPa may be sufficient for small batches where tablets are not subjected to considerable mechanical stresses.

The tableting behavior of habit-modified 5-ASA powders is shown in Figure 6. All habit-modified 5-ASA powders formed intact tablets. No capping (separation of lower or upper segment of tablet horizontally) or lamination (splitting of a

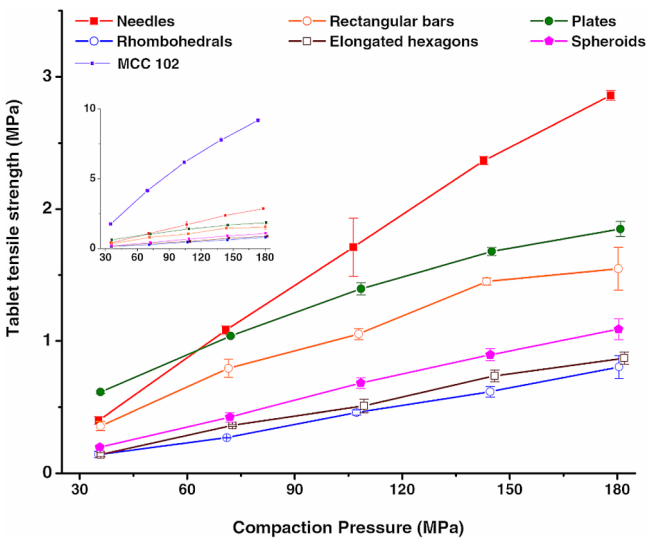

Figure 6. Tablet tensile strength (n = 3, mean ± SD) as a function of compaction pressure for six crystal habits of 5-ASA. The inset displays tabletability comparison with microcrystalline cellulose PH 102 (MCC 102) included as a reference. The axes title in the inset is same as in the main plot.

DOI: 10.1021/acs.oprd.6b00434
Org. Process Res. Dev. XXXX, XXX, XXX−XXX

tablet into two or more distinct horizontal layers) was observed up to the maximum pressure studied (180 MPa). The tabletability of 5-ASA was also compared with MCC 102, which was included as a reference. Tabletabilities of all habit-modified 5-ASA were significantly lower than that of MCC 102 in the pressure range 35−180 MPa (Figure 6, inset). Among six habits, needles produced the strongest tablets at pressures greater than 70 MPa, but at the lowest pressure (35 MPa), plates produced slightly stronger tablets.

As mentioned before, 5-ASA crystallizes out in needles from its typical crystallization conditions. Of six habits studied here, tabletability assessment showed changing the crystal habit from needles to other habits did not result in improved tableting behavior. When a general guide[32] for adequate tensile strength is considered, needles are the best crystal habit followed by plates for 5-ASA. More isotropic shapes (spheroids, elongated hexagons, and rhombohedrals) produced comparatively weaker tablets.

3.4. Optimal Crystal Habit. Processability assessment indicated that not a single crystal habit possessed the best flow properties and tabletability, which is illustrated in Figure 7 in

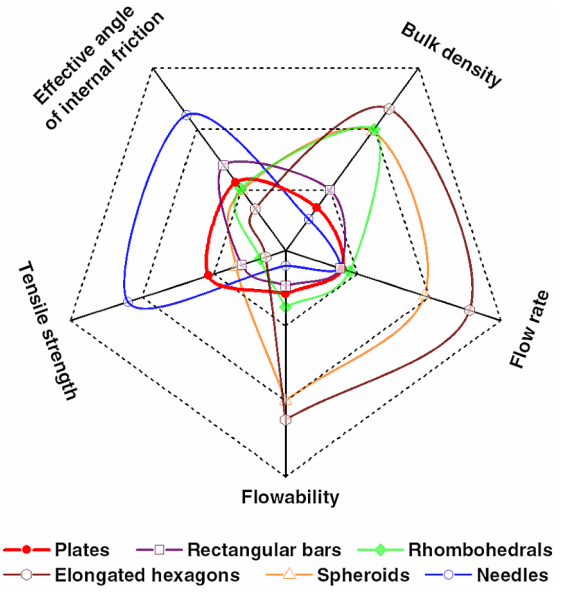

Figure 7. Spider chart illustrating flow indicators and tabletability for six crystal habits of 5-ASA. Each arm is scaled independently. Ideally, the best habit will have all indicator values toward the edges except the "effective angle of internal friction", which should be closer to the center. Data for this chart are also in Table SI 2.

the form of a spider chart. Although needles resulted in relatively strong tablets, they were poorly flowing and had a low flow rate, suggesting further processing steps, such as granulation, needed to process them better downstream. The opposite was observed with spheroids and elongated hexagons. They were free-flowing, had a relatively high flow rate and bulk density, but produced comparatively weak tablets. When both flowability and tabletability were considered, the plate-like habit showed a good compromise and is the optimal crystal habit for efficient downstream processing. The plate-like habit of 5-ASA was easy flowing (ff_c = 5.8) and had a flow rate of 7 mg/s. It produced tablets with a tensile strength of 1.4 MPa at a solid fraction of 0.9, close to that of the general guidance value.[32]

4. CONCLUSIONS

Downstream processability of six representative crystal habits of a model API was assessed in the context of direct compression. Free-flowing habits, namely, spheroids and elongated hexagons, performed poorly when compared to needles in tabletability assessment. When both flowability and tabletability were considered, the plates were identified as an optimal habit for downstream processing. Understanding optimal API processing properties can provide an advantage when trying to build those properties into the API. Carrying out processability assessment early on during product development may help identify optimal habit(s) for efficient processing, where the aim in general is to find a good enough rather than perfect crystal habit. This is feasible with the availability of material-sparing instruments. For instance, in our case, processability (both flowability and tabletability) was assessed using 5−10 g of habit-modified powders depending on the bulk density.

■ ASSOCIATED CONTENT

Supporting Information

The Supporting Information is available free of charge on the ACS Publications website at DOI: 10.1021/acs.oprd.6b00434.

Illustration and definitions of crystal shape and size-related parameters, schematics of ring shear tester and flow rate analyzer, flow and tabletability indicator data for the spider chart, and SEM image of MCC 102 (reference powder) (PDF)

■ AUTHOR INFORMATION

Corresponding Author

*Tel: +45 35336585; e-mail: jukka.rantanen@sund.ku.dk.

ORCID

Nawin Pudasaini: 0000-0003-4631-4323
Pratik P. Upadhyay: 0000-0002-2541-9559
Jukka Rantanen: 0000-0002-8211-5607

Notes

The authors declare the following competing financial interest(s): This paper is related to the principal product of Syntese A/S, and the research is a result of the Ph.D. work of N.P., which is partly sponsored by Syntese A/S. S.U.H. and C.R.P. are employed at Syntese A/S.

■ ACKNOWLEDGMENTS

We acknowledge financial support from Syntese A/S (Denmark) and the Department of Pharmacy, Graduate School of Health and Medical Sciences, University of Copenhagen (Denmark).

■ REFERENCES

(1) Davies, P. Oral solid dosage forms. In *Pharmaceutical preformulation and formulation: a practical guide from candidate drug selection to commercial dosage form*; Gibson, M., Ed.; Informa Healthcare: New York, 2009; Vol. *199*, p 367.
(2) Leane, M.; Pitt, K.; Reynolds, G. *Pharm. Dev. Technol.* **2015**, *20* (1), 12−21.
(3) McCormick, D. *Pharm. Technol.* **2005**, *1*, 52−62.
(4) Shangraw, R. F. *Pharm. Dosage Forms: Tablets* **1989**, *1*, 195−246.
(5) Chatterjee, S. FDA perspective on continuous manufacturing. Presented at IFPAC Annual Meeting, Baltimore, MD, 2012. http://www.fda.gov/downloads/AboutFDA/CentersOffices/OfficeofMedicalProductsandTobacco/CDER/UCM341197.pdf (accessed November 21, 2016).

DOI: 10.1021/acs.oprd.6b00434
Org. Process Res. Dev. XXXX, XXX, XXX−XXX

(6) Tezyk, M.; Milanowski, B.; Ernst, A.; Lulek, J. *Drug Dev. Ind. Pharm.* **2016**, *42* (8), 1195−1214.
(7) Adobes-Vidal, M.; Maddar, F. M.; Momotenko, D.; Hughes, L. P.; Wren, S. A.; Poloni, L. N.; Ward, M. D.; Unwin, P. R. *Cryst. Growth Des.* **2016**, *16* (8), 4421−4429.
(8) Modi, S. R.; Dantuluri, A. K.; Puri, V.; Pawar, Y. B.; Nandekar, P.; Sangamwar, A. T.; Perumalla, S. R.; Sun, C. C.; Bansal, A. K. *Cryst. Growth Des.* **2013**, *13* (7), 2824−2832.
(9) Banga, S.; Chawla, G.; Varandani, D.; Mehta, B.; Bansal, A. K. *J. Pharm. Pharmacol.* **2007**, *59* (1), 29−39.
(10) Kumar, S.; Chawla, G.; Bansal, A. K. *Pharm. Dev. Technol.* **2008**, *13* (6), 559−568.
(11) Overgaard, A.; Moller-Sonnergaard, J.; Christrup, L.; Hojsted, J.; Hansen, R. *Pharm. World Sci.* **2001**, *23* (5), 185−188.
(12) Rohl, A. L. *Curr. Opin. Solid State Mater. Sci.* **2003**, *7* (1), 21−26.
(13) Lovette, M. A.; Browning, A. R.; Griffin, D. W.; Sizemore, J. P.; Snyder, R. C.; Doherty, M. F. *Ind. Eng. Chem. Res.* **2008**, *47* (24), 9812−9833.
(14) Hou, H.; Sun, C. C. *J. Pharm. Sci.* **2008**, *97* (9), 4030−4039.
(15) Bruno, I. J.; Cole, J. C.; Edgington, P. R.; Kessler, M.; Macrae, C. F.; McCabe, P.; Pearson, J.; Taylor, R. *Acta Crystallogr., Sect. B: Struct. Sci.* **2002**, *58* (3), 389−397.
(16) Banic-Tomisic, Z.; Kojic-Prodic, B.; Sirola, I. *J. Mol. Struct.* **1997**, *416* (1), 209−220.
(17) Groom, C. R.; Bruno, I. J.; Lightfoot, M. P.; Ward, S. C. *Acta Crystallogr., Sect. B: Struct. Sci., Cryst. Eng. Mater.* **2016**, *72* (2), 171−179.
(18) Laitinen, N.; Rantanen, J.; Laine, S.; Antikainen, O.; Rasanen, E.; Airaksinen, S.; Yliruusi, J. *Chemom. Intell. Lab. Syst.* **2002**, *62* (1), 47−60.
(19) Lindberg, N.; Lundstedt, T. *Drug Dev. Ind. Pharm.* **1995**, *21* (9), 987−1007.
(20) Jenike, A. W. *Storage and flow of solids*; University of Utah: Salt lake City, UT, 1964; Vol. *53*, p 198.
(21) Seppala, K.; Heinamaki, J.; Hatara, J.; Seppala, L.; Yliruusi, J. *AAPS PharmSciTech* **2010**, *11* (1), 402−408.
(22) ASTM International. ASTM D6773-16, *Standard Test Method for Bulk Solids Using Schulze Ring Shear Tester*; West Conshohocken, PA, 2016.
(23) Fell, J.; Newton, J. *J. Pharm. Sci.* **1970**, *59* (5), 688−691.
(24) Myerson, A.; Ginde, R. Crystals, Crystal growths and Nucleation. In *Handbook of Industrial Crystallization*; 2nd ed.; Myerson, A., Ed.; Butterworth-Heinemann: Woburn, MA, 2002; pp 41−42.
(25) Sun, C.; Grant, D. J. W. *Pharm. Res.* **2001**, *18* (3), 274−280.
(26) Schulze, D. *Powders and bulk solids: Behaviour, Characterization, Storage and Flow*; Springer 2008; p 75−110.
(27) Sun, C. C. *Powder Technol.* **2016**, *289*, 104−108.
(28) Sirola, I.; Luksic, J.; Simunic, B.; Kujundzic, N. *J. Cryst. Growth* **1997**, *181* (4), 403−409.
(29) Sogaard, S. V.; Pedersen, T.; Alleso, M.; Garnaes, J.; Rantanen, J. *Int. J. Pharm.* **2014**, *475* (1), 315−323.
(30) Hirschberg, C.; Sun, C. C.; Rantanen, J. *J. Pharm. Biomed. Anal.* **2016**, *128*, 462−468.
(31) Sun, C. C.; Hou, H.; Gao, P.; Ma, C.; Medina, C.; Alvarez, F. J. *J. Pharm. Sci.* **2009**, *98* (1), 239−247.
(32) Pitt, K. G.; Heasley, M. G. *Powder Technol.* **2013**, *238*, 169−175.

DOI: 10.1021/acs.oprd.6b00434
Org. Process Res. Dev. XXXX, XXX, XXX−XXX